International Journal of Scientific Research Updates

Journal homepage: https://orionjournals.com/ijsru/

ISSN: 2783-0160 (Online)

(RESEARCH ARTICLE)

Feasibility of MPC enhanced couch as SRS/SBRT Pretreatment QA

Aime M Gloi *

Department of Radiation Oncology, Modesto California, USA.

International Journal of Scientific Research Updates, 2023, 06(02), 001–016

Publication history: Received on 06 September 2023; revised on 17 October 2023; accepted on 20 October 2023

Article DOI: https://doi.org/10.53430/ijsru.2023.6.2.0064

Abstract

Purpose: The purpose of this study was to investigate the feasibility of using the Winston-Lutz (WL) interchangeability with a Machine Performance Check-enhanced couch for pretreatment quality assurance (QA) of stereotactic radiotherapy (SRS) and stereotactic body radiation therapy (SBRT). The study employed the MPC with an electronic portal imaging device (EPID) to carry out geometric checks and verify the radiation isocenter. The isocenter size was assessed using the MultiMet cube and the MPC-enhanced couch module for SRS/SBRT pretreatment QA.

Methods: The isocenter size of the MPC-enhanced couch module was compared to the WL measurements of the MultiMet cube. Measurements were taken at various gantry, collimator, and couch angles over a period of one month. The data from the cube were evaluated using PIPSRO and MultiMet (MMWL), including the offset targets. Various statistical tests were performed to evaluate the agreement, normality, separability, sensitivity, and specificity between the two methods.

Results: The results showed isocenter sizes of 0.273 ± 0.065 mm, 0.293 ± 0.010 mm, and 0.209 ± 0.070 mm for PIPSPRO, MPC, and MMWL, respectively. The average bias was -0.0639 ± 0.1061 mm between MMWL and PIPSPRO, -0.0837 ± 0.0688 mm between MMWL and MPC, and 0.0198 ± 0.0696 mm between MPC and PIPSPRO. A Shapiro-Wilk test revealed no significant departure from normality for all tests and showed satisfactory discrimination through the area under the curve (AUC). A paired t-test analysis revealed a statistically significant difference between the mean isocenter size of the MPC and WL (MMPWL: $t = 5.654$, $df = 29$, $p < 0.001$; PIPSPRO: $t = -1.483$, $DF = 29$, $p = 0.1488$), and there was no significant difference within the WL test ($t = 3.008$, $DF = 29$, $p = 0.0054$).

Conclusion: Despite the statistical test results, there was agreement between the MPC and WL radiation isocenter size that was within the requirement of the AAPM TG 142 tolerance (±1.0 mm). The MPC proved to be accurate, reproducible, and consistent throughout the measurements, making it an appropriate and effective pretreatment QA tool for SRS/SBRT.

Keywords: Winston-Lutz; Machine Performance Check-enhanced couch; Stereotactic radiotherapy (SRS); Stereotactic body radiation therapy (SBRT)

1 Introduction

In this study, we assessed the radiation isocenter defined by the gantry, collimator, and couch rotation center using both EPID with the WL approach and the machine performance check (MPC) enhanced couch module. We specifically evaluated the off-axis WL for planned radiation in the high-dose regions at off-axis positions. A medical linear accelerator (linac) requires both mechanical and radiation isocenters for successful stereotactic radiosurgery (SRS) and stereotactic body radiation therapy (SBRT). According to the AAPM TG142 [1] guidelines, a ±1 mm deviation for both treatments is recommended to protect surrounding normal tissues, particularly in the brain, spine, and lung lesions.

* Corresponding author: Aime M Gloi

The widely used WL [2] method is commonly employed in linac quality assurance (QA) to verify the coincidence of mechanical and radiation isocenters. This method offers a simple, effective, and reproducible procedure for determining the gantry, collimator, and couch isocenter, primarily for aligning lesions near the isocenter. However, because of uncertainties in couch rotation and small target inaccuracies away from the isocenter, this method is not suitable for lesions treated with a multi-target single isocenter approach. Szweda et al. [3] analyzed isocenter data based on three different phantom measurements and concluded that reducing the size of the sphere containing radiation at the MV isocenter would minimize systematic errors. Eagle et al. [4] proposed the use of an off-axis distance to reduce sources of error and achieve more accurate results in the isocentric WL test. Likewise, Gao et al. [5] demonstrated the use of on-board imaging (OBI) and EPID systems with the IsoCal phantom, which showed consistent accuracy comparable to WL tests using a Varian cubic phantom. Therefore, as the utilization of SRS and SBRT continues to increase, it is essential to improve the efficiency of quality assurance (QA). In this study, we evaluated the radiation isocenter defined by the gantry, collimator, and couch rotation center using both EPID with the WL approach and the machine performance check (MPC) enhanced couch module. We particularly assessed the off-axis WL for planned radiation in the high-dose regions at off-axis positions.

2 Material and methods

In this study, the verification of the isocenter was performed in multiple steps. Firstly, the WL test was conducted by acquiring EPID images of the MultiMet-WL (MMWL) cube (Sun Nuclear Corporation, Melbourne, Florida, USA) placed on the treatment delivery couch at the isocenter (Figure 1a) of the TrueBeam™ EDGE™ linac (Varian Medical Systems, Palo Alto, CA) at various gantry, collimator, and couch angles (Table 1).

Table 1 Winston–Lutz gantry, couch, and collimator angles for PIPSPRO procedures

Gantry	Couch	Collimator
180	0	160
90	90	0
270	270	0
0	90	90
0	45	45
0	315	315
0	270	270

Figure 1 (a) Setup of the MultiMet phantom on the treatment couch with the machine reference at [0, 0, 0] coordinates

Figure 1 (b) Schematic of the MultiMet phantom

As shown in Figure 1b, the cube is an acrylic block measuring 8.5 × 8.5 × 12.75 mm and contains six tungsten carbide spheres with a diameter of 5.000 ± 0.025 mm. The WL analysis was carried out using PIPSPROTM software (Standard Imaging Middleton, WI, USA). Subsequently, radiation exposures were made on the same cube using the parameters listed in Table 2, along with enclosed MLC plans, to check for both isocenter and off-axis targets (1–5). By visualizing the off-axis spatial discrepancies, it was possible to establish limitations on the maximum distance between targets based on recommended guidelines. The data were then analyzed using the MMWL platform.

Table 2 This work considers various combinations of gantry, collimator, and couch angles

Gantry	Couch	Collimator
0	0	0
0	0	90
0	0	270
0	90	0
0	270	0
90	0	90
180	0	90
270	0	90

Finally, the Isocal phantom, a white hollow Delrin cylinder with 16 embedded tungsten bearing balls (BBs) was positioned on the mount assembly (Figure 2). The Enhanced Couch Geometry Check (ECGC) module was performed with wider couch axes of travel (90, 45, 315, and 270°). The machine isocenter for all these procedures was assigned to the [0, 0, 0] coordinate of the phantom.

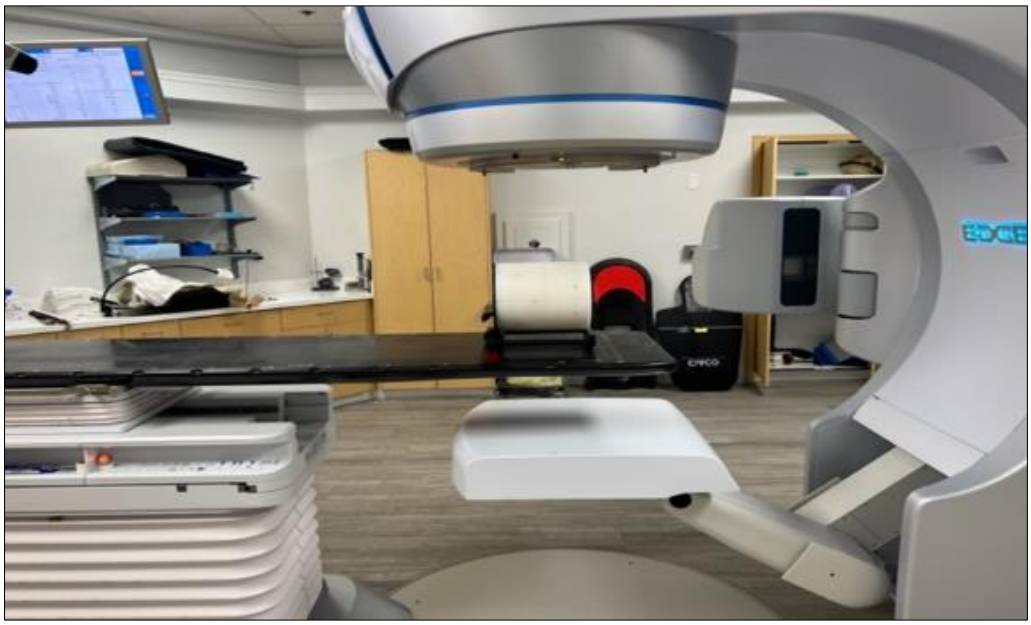

Figure 2 The Isocal phantom mounted to the couch during an isocenter verification test

2.1 Data analysis

The WL test enabled the determination of the diameter of the sphere containing the radiation isocenter. In this report, two commercially available software products were used for the WL test:

2.1.1 PIPSPRO:

The PIPSPRO analysis was based on singular value decomposition (SVD), where the offset of the head frame from the optimal target location is given by-Equation (1).

$$\begin{pmatrix} dU \\ dV \end{pmatrix} = \begin{pmatrix} cos\emptyset & -sin\emptyset & 0 \\ cos\theta\, sin\emptyset & cos\theta\, cos\emptyset & -sin\theta \end{pmatrix} \times \begin{pmatrix} -dY \\ dX \\ dZ \end{pmatrix} \quad \text{.....(1)}$$

2.1.2 MMWL

The DICOM images from the EPID were examined through the beam edges and sphere stamps. The centroids of the spheres and beams were then calculated. For gantry (q) and couch (f) angles, 2D EPID coordinates could be mapped to the patient frame using the transformation equation provided by:

$$\begin{pmatrix} u \\ v \end{pmatrix} = \begin{pmatrix} cos(\theta)cos(\phi) & -cos(\theta)sin(\phi) & sin(\theta) \\ sin(\phi) & cos(\phi) & 0 \end{pmatrix} \times \begin{pmatrix} \Delta_{VERT} \\ \Delta_{LAT} \\ -\Delta_{AP} \end{pmatrix} \quad \text{.....(2)}$$

2.1.3 MPC

Additionally, the MPC evaluated parameters by using an MV/kV image series generated based on an embedded computational model to derive radiation isocenter size, coincidence of MV/kV isocenters, and accuracy of the collimator. The positions of the jaw, MLC leaves, and couch, including yaw, pitch, and roll, were also determined.

2.2 Statistics

Descriptive statistics (Medcalc@ Statistical Software version 22.009 Ltd., Ostend, Belgium) were employed to evaluate the difference between methods and identify the limit of agreement. A Shapiro-Wilk test of normality was conducted to determine whether the difference between methods for the isocenter evaluation was normally distributed. A paired Student's two-tailed t-test was used to compare the isocenter size of different methods. Bland-Altman plots were utilized to further examine the difference between methods. The appropriateness between imaging platforms was assessed with action levels defined as ≥ 0.75 mm for "warning" and ≥ 1 mm for "fail" based on the AAPM TG142.

3 Results

Figure 3 illustrates the set of beams projected at target #1 (Gantry = 180°; Col = 90°; Couch = 0°) for 2 x 2 cm^2 beams delivered at the isocenter using portal dosimetry imaging. The 3D position of the 6 targets allows for the evaluation of isocenter offset on a dimensional plane, as well as roll, pitch, and yaw. The figures indicate the error as a function of distance from the isocenter and the linac position.

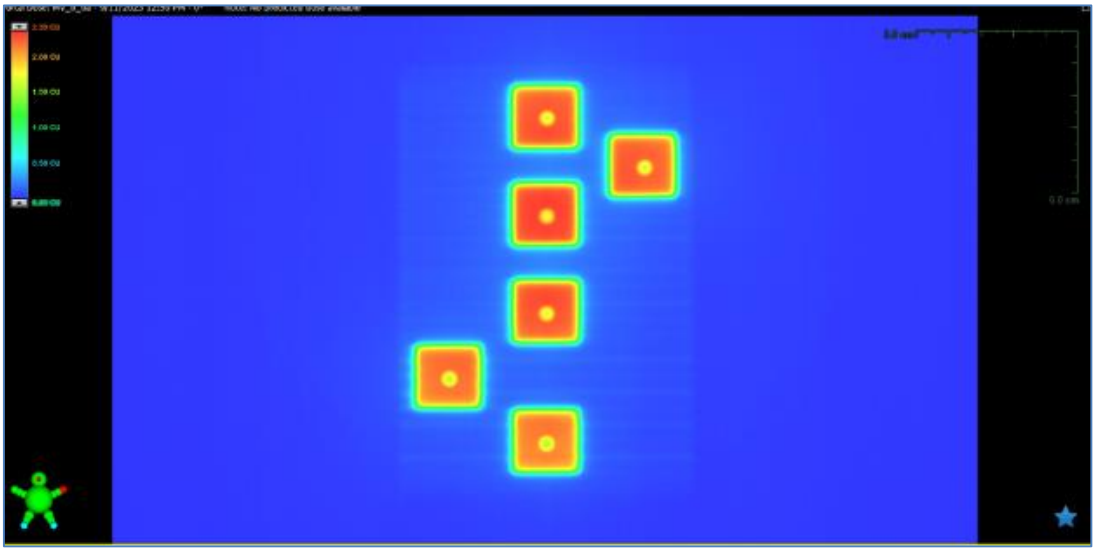

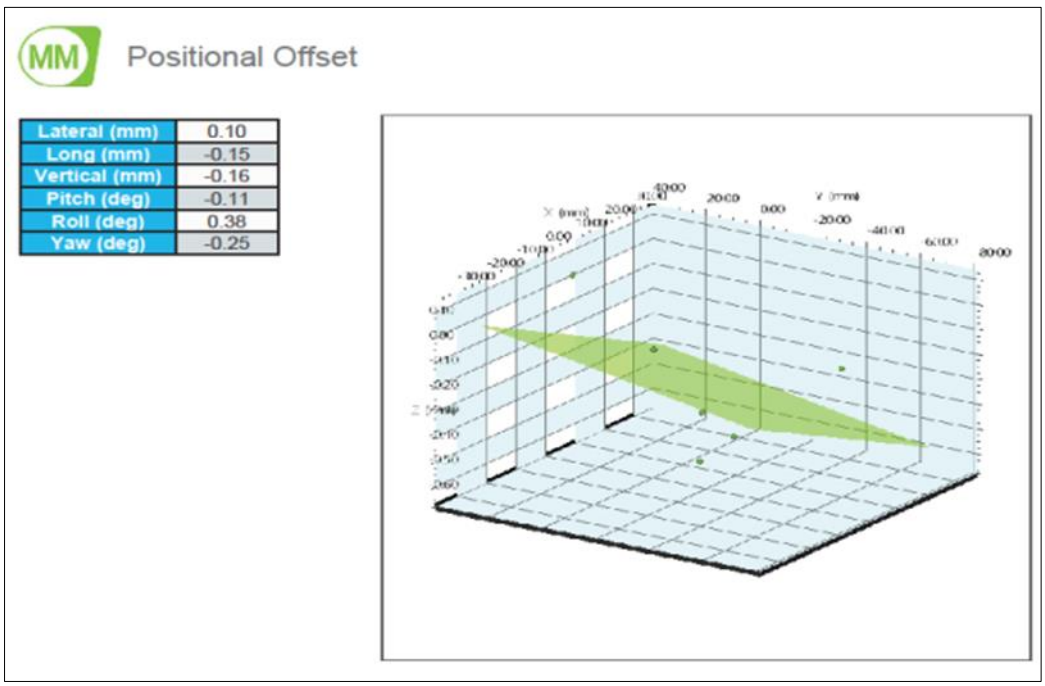

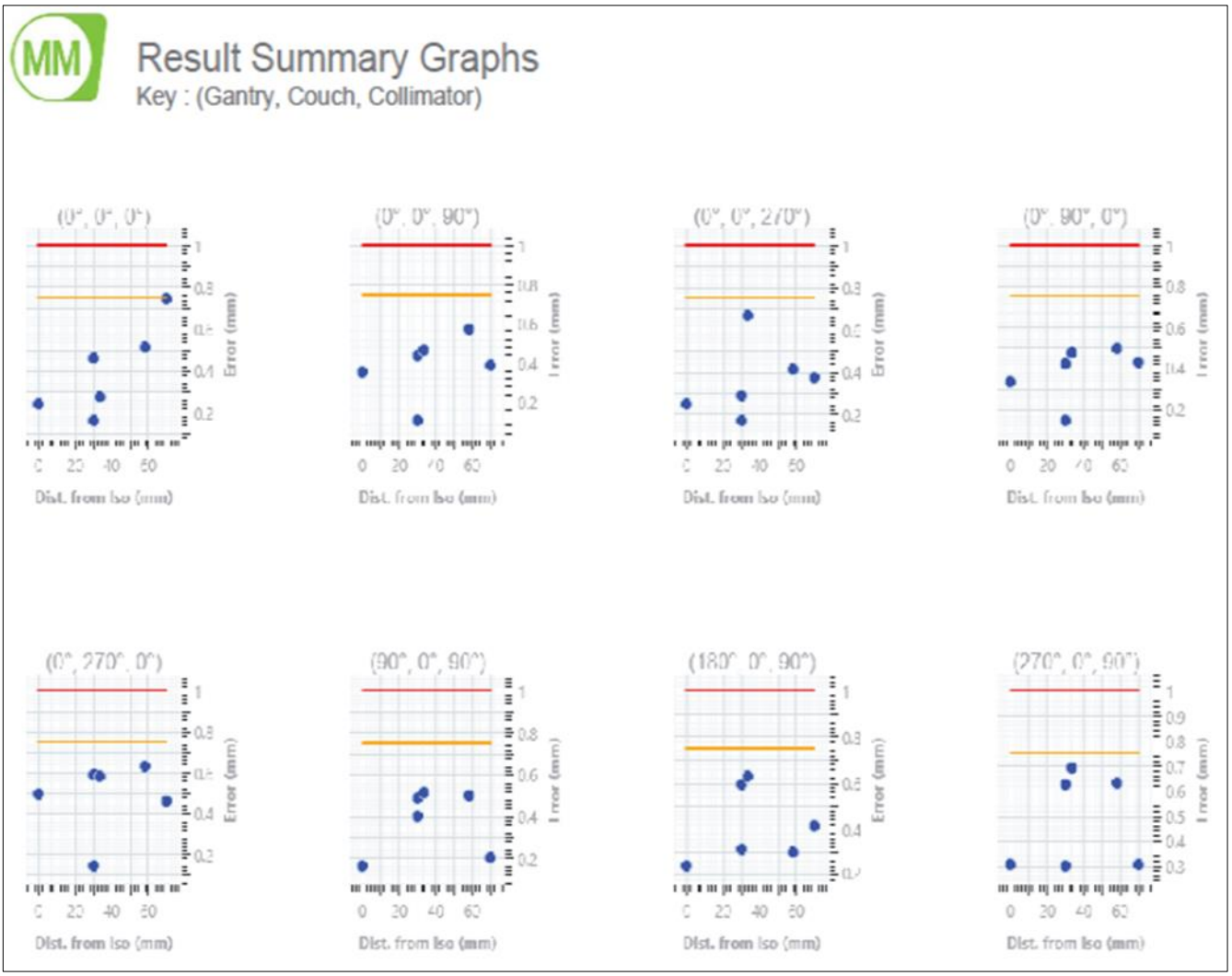

Figure 3 Winston-Lutz (WL) analysis was conducted to assess the pitch, roll, and yaw of the phantom relative to the radiation isocenter. The analysis was based on the offset targets in their 3D locations. Each subfield produced a 2 × 2 cm2 radiation field with a metallic BB centered in the fields

Figure 4 presents an example of acquired EPID images analyzed using MMWL and PIPSPRO. The software detects the location of the BBs from the cross-sectional profiles within the subfield and measures the distances of the field edges to the center of the BBs to determine the offset from the center for all 6 subfields. The offset is measured between the blue circle with crosshairs, the center of mass of each BB, and the center of the 2 x 2 cm^2 radiation field for each gantry, collimator, and couch position.

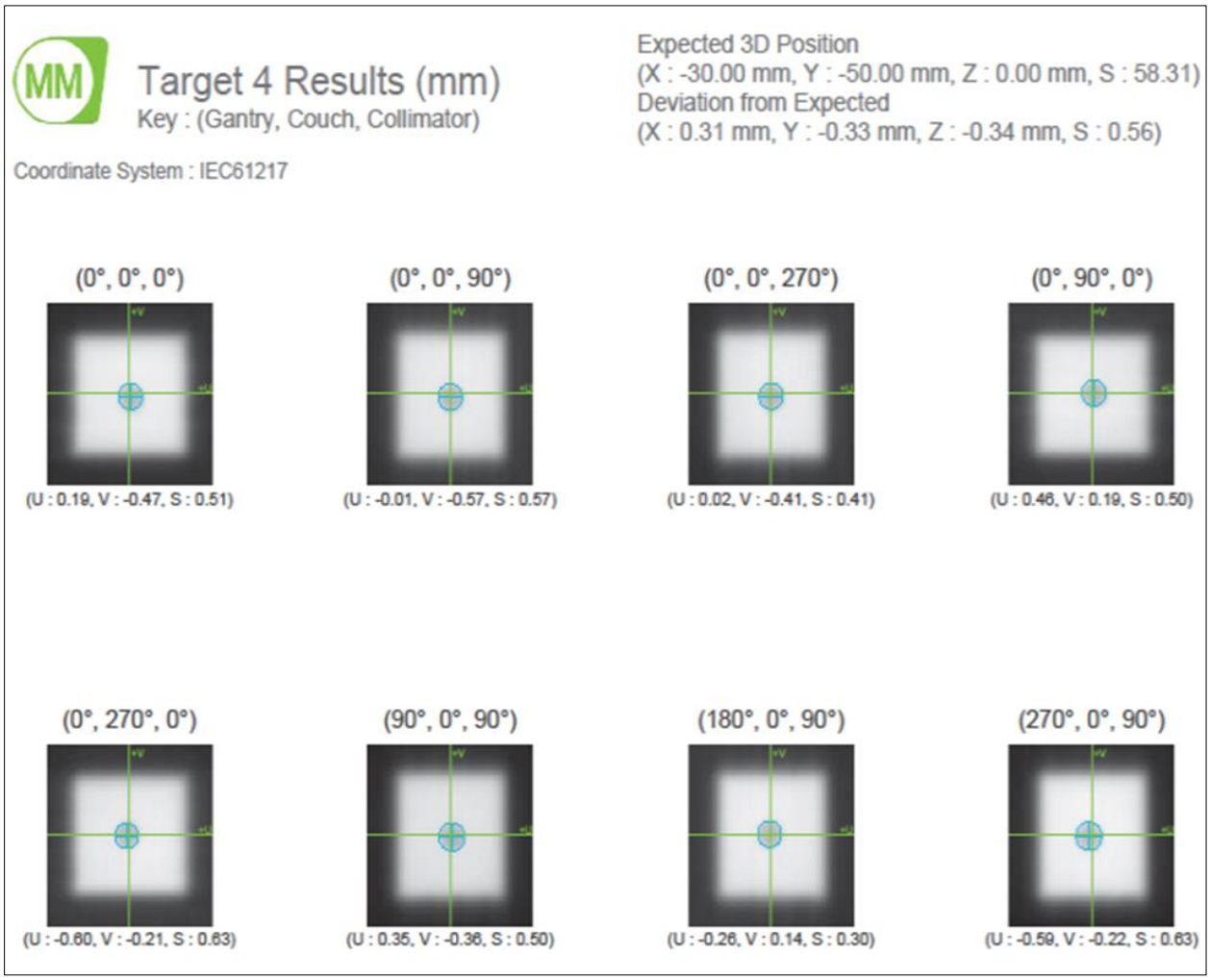
Target 4 Results (mm)
Key : (Gantry, Couch, Collimator)
Expected 3D Position
(X : -30.00 mm, Y : -50.00 mm, Z : 0.00 mm, S : 58.31)
Deviation from Expected
(X : 0.31 mm, Y : -0.33 mm, Z : -0.34 mm, S : 0.56)
Coordinate System : IEC61217
(0°, 0°, 0°)
(U : 0.19, V : -0.47, S : 0.51)
(0°, 0°, 90°)
(U : -0.01, V : -0.57, S : 0.57)
(0°, 0°, 270°)
(U : 0.02, V : -0.41, S : 0.41)
(0°, 90°, 0°)
(U : 0.46, V : 0.19, S : 0.50)
(0°, 270°, 0°)
(U : -0.60, V : -0.21, S : 0.63)
(90°, 0°, 90°)
(U : 0.35, V : -0.36, S : 0.50)
(180°, 0°, 90°)
(U : -0.26, V : 0.14, S : 0.30)
(270°, 0°, 90°)
(U : -0.59, V : -0.22, S : 0.63)

MMWL

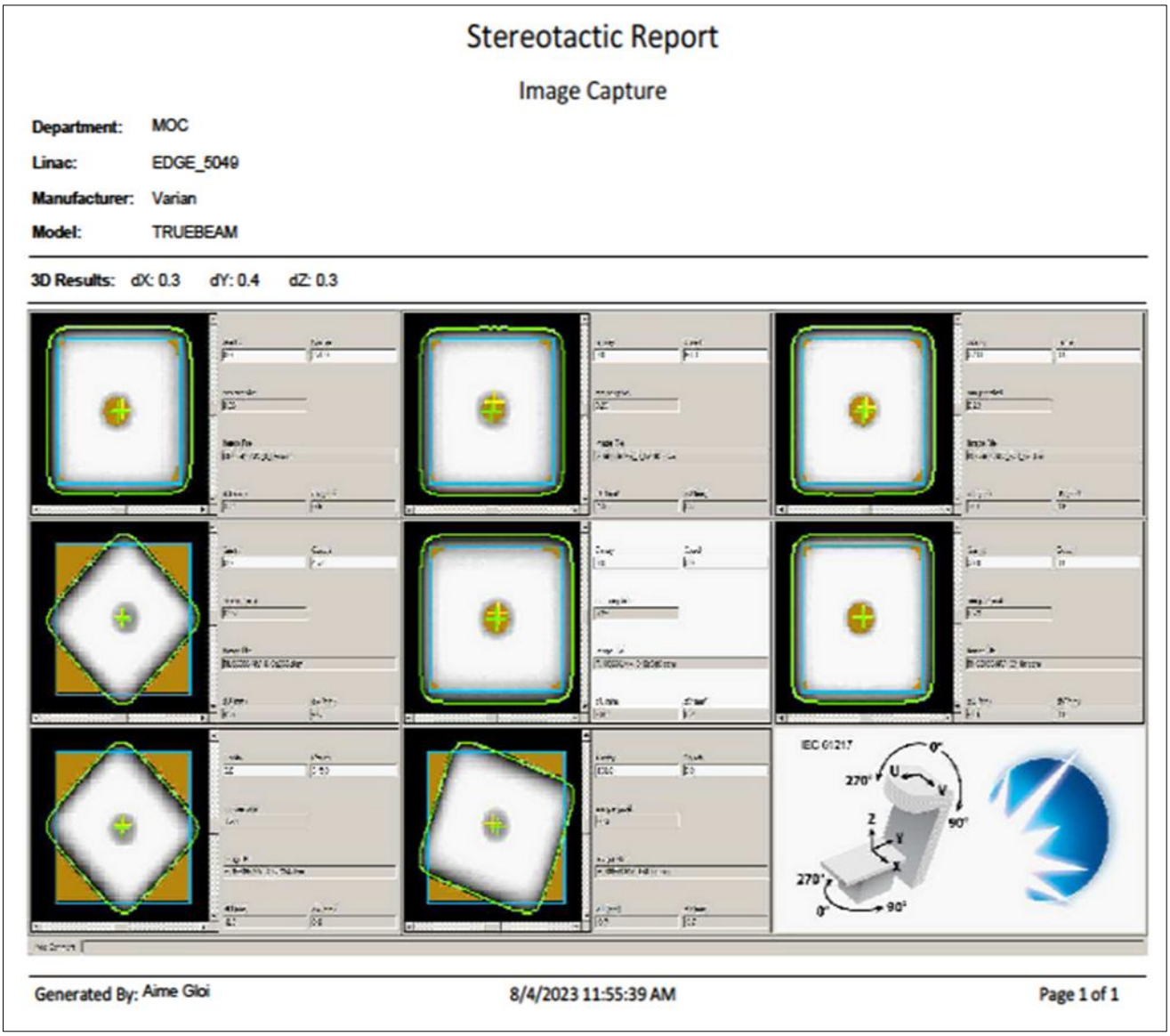

PIPSPRO

Figure 4 An example of the 2x2 cm2 beams delivered at the isocenter for a Varian TrueBeam Edge is shown. The errors for MMWL and PIPSPRO are plotted as a function of distance from the isocenter

Figure 5 displays the isocenter size over a month as determined by PIPSPRO, MMWL for a cube, and MPC. The mean and standard deviation are presented in a box-whisker plot, showing the BB location errors as a function of distance from the isocenter (Figure 6). The summarized results for PIPSPRO, MMWL, and MPC are 0.2736 ± 0.0657 mm, 0.2096 ± 0.0703 mm, and 0.2930 ± 0.0105 mm, respectively. The results indicate that the WL is smaller than that of MPC and appears to vary and be less consistent, while the data points for MPC are clustered, suggesting stability.

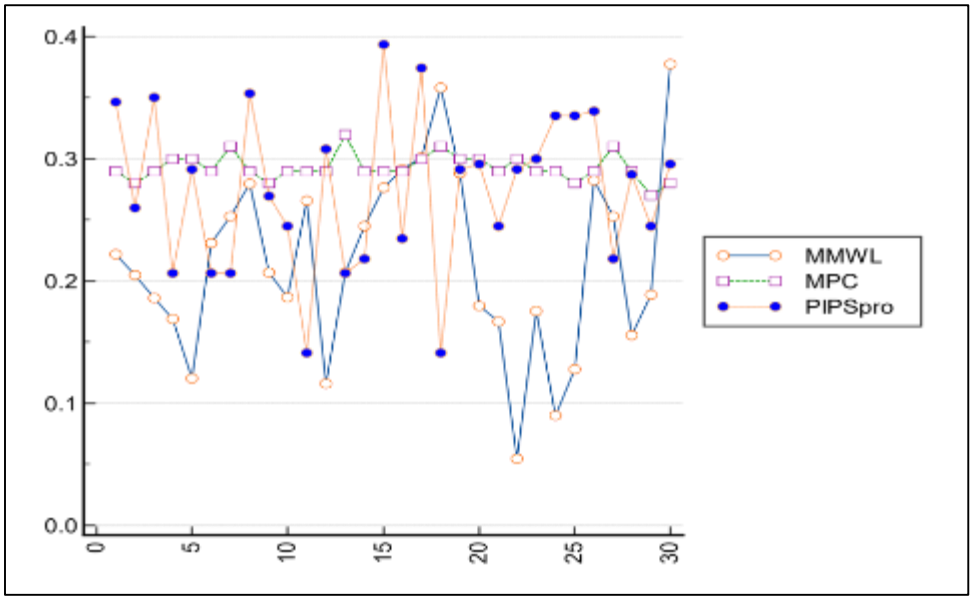

Figure 5 The average values of the isocenter found for MMWL, PIPSPRO, and MPC (enhanced couch) were analyzed using tolerance limits of 0.75 mm and 1 mm (x= days; y=displacement in mm)

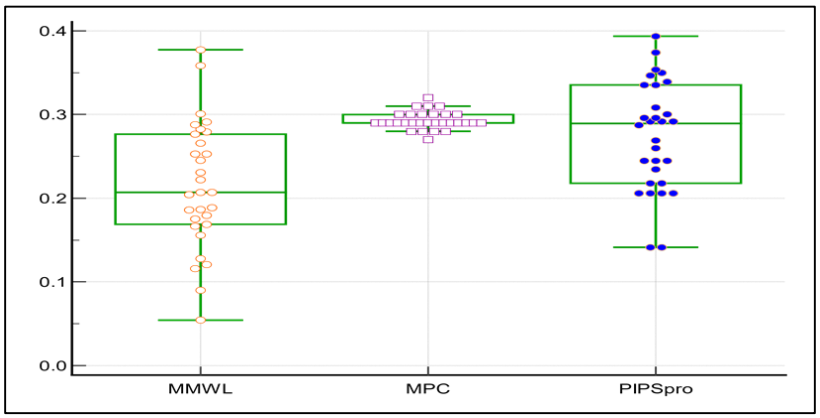

Figure 6 A Box-Whisker's plot was created to display the isocenter test data obtained over a month for MMWL, PIPSPRO, and MPC (Y axis =displacement in mm)

Figure 7 provides a three-dimensional visualization of the measured isocenter size location. All measurements are within the AAPM's 1 mm tolerance for the mechanical isocenter for all methods and phantoms used.

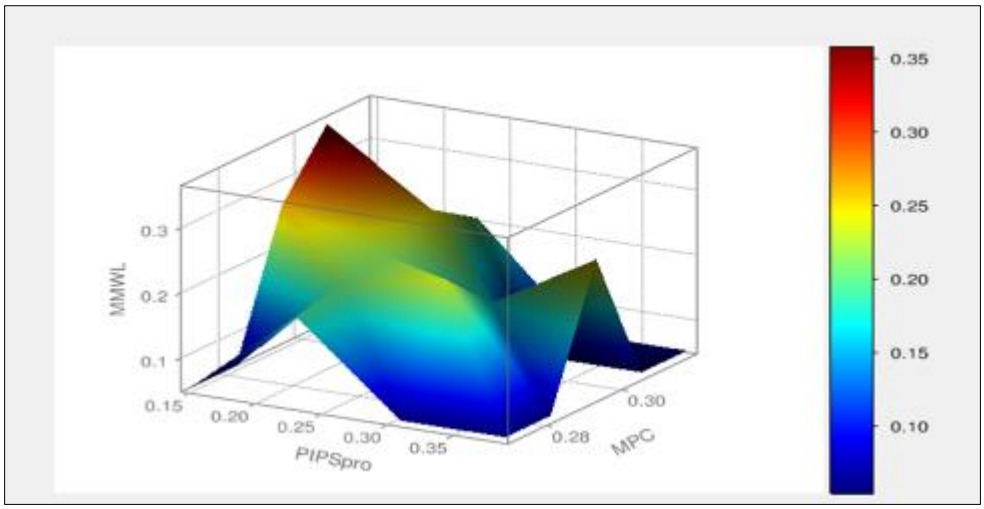

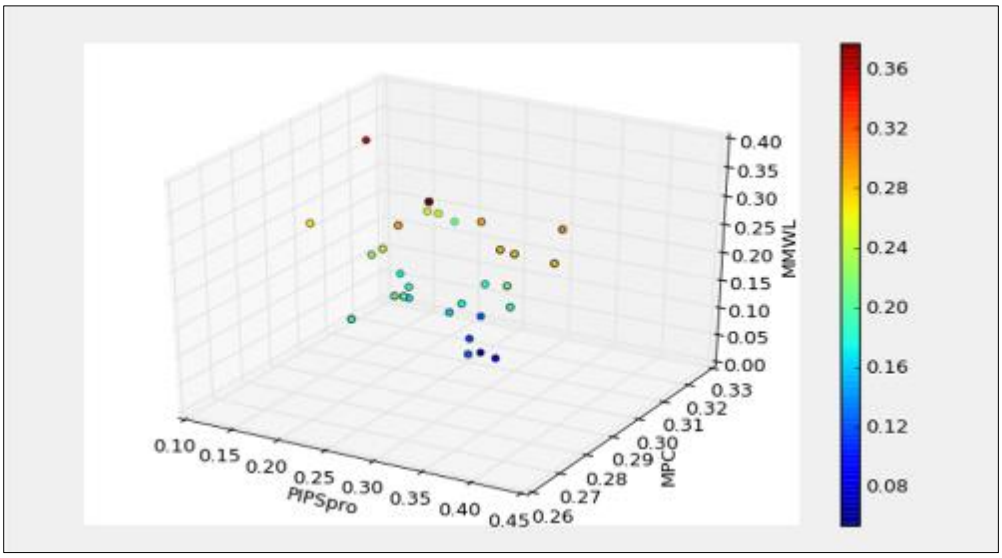

Figure 7 The size of the isocenter was measured in 3D over 30 days using MMWL, PIPSPRO, and MPC

The agreement between WL and MPC, as well as within WL isocenter size measurements, was evaluated using Bland-Altman analysis, which included a measure of bias (mean difference) with 95% limits of agreement (LOA) (Figure 8). Additionally, the mean value of measurement errors was shown to be approximately zero indicating no significant differences in measurements between the two methods in accordance with AAPM TG 142 tolerance.

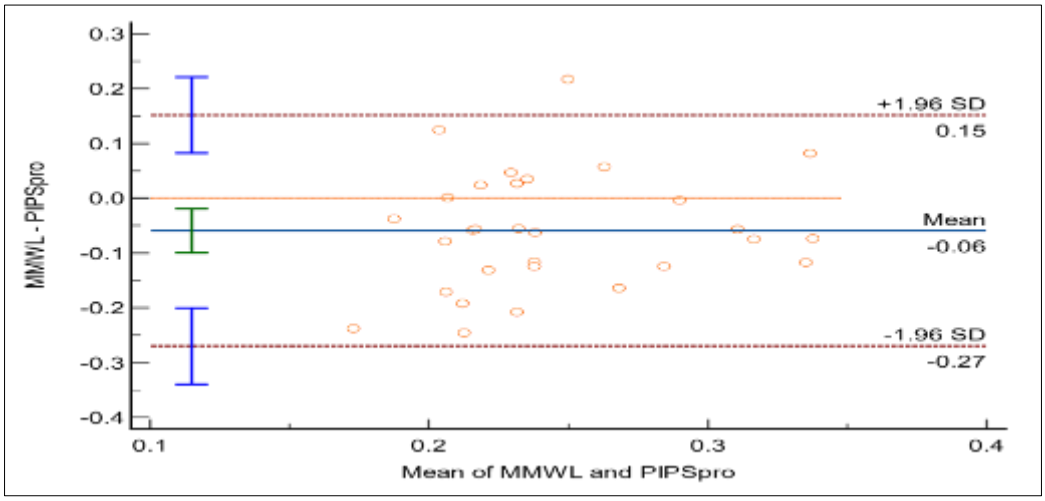

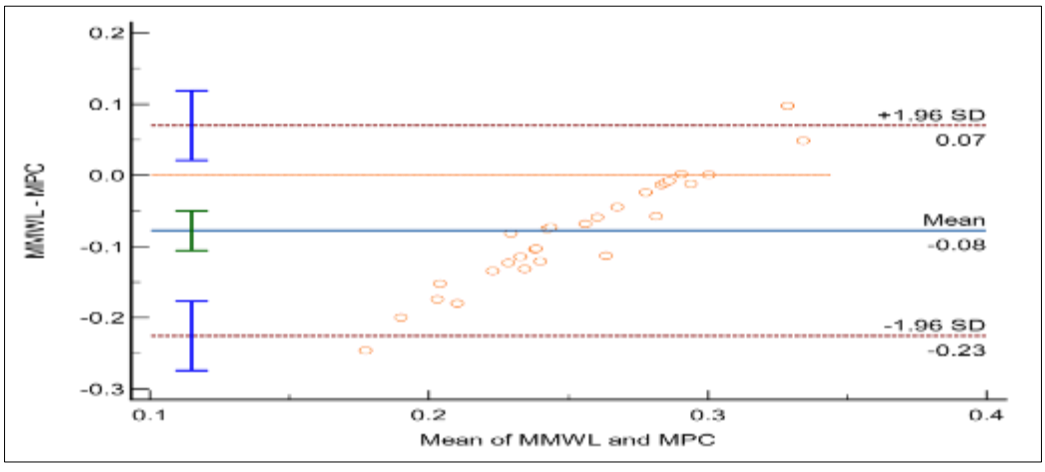

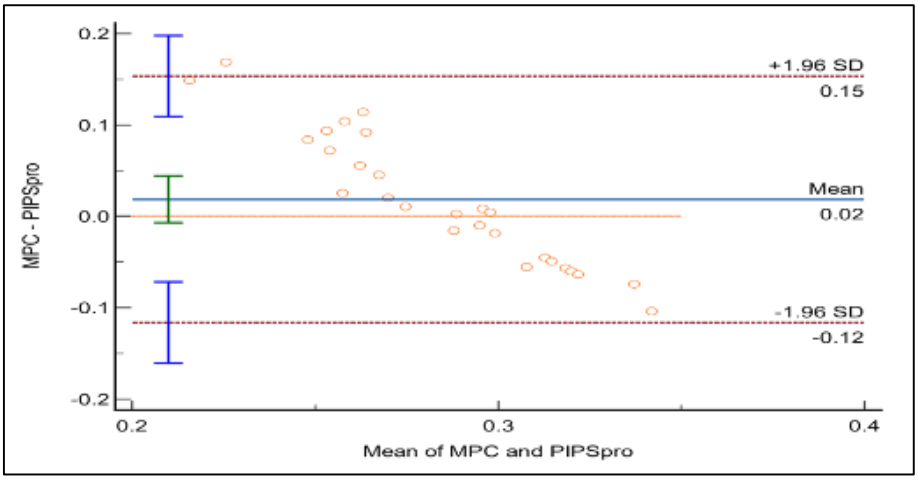

Figure 8 Bland-Altman plots were used to compare the agreement between MPC and WL. The difference in readings was plotted against the average reading. Perfect agreement would result in all points lying on the horizontal zero line

3.1 Statistics

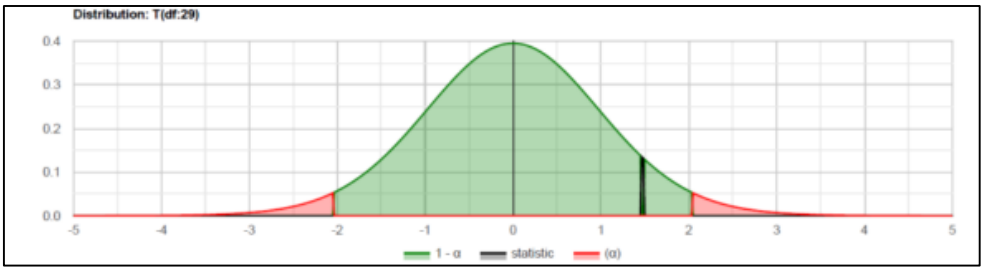

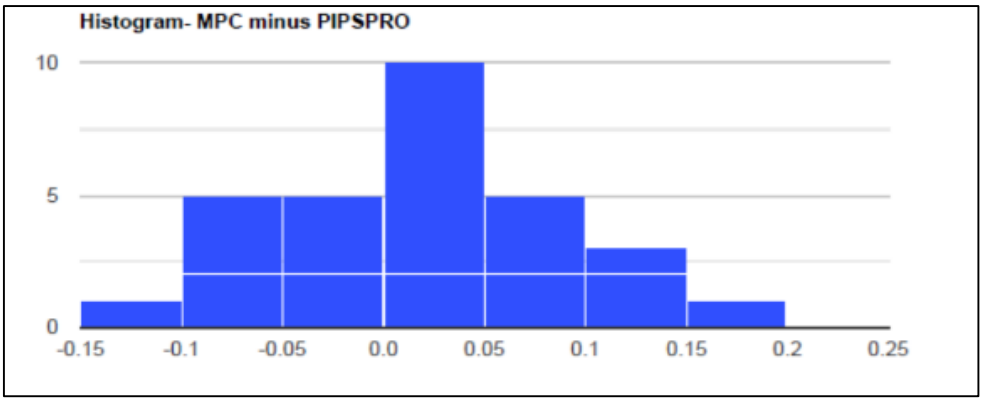

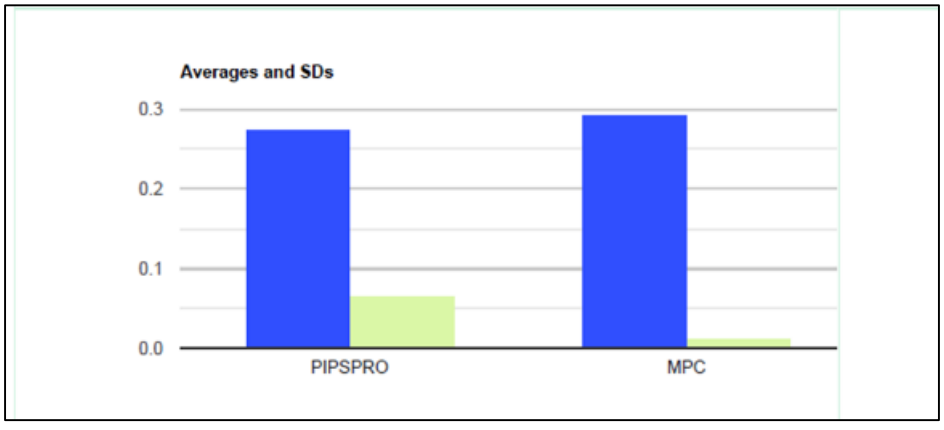

Figure 9a The distribution of the analysis of the isocenter size difference-between MPC and PIPSPRO is shown

A paired sample t-test was performed to determine if there was a difference between WL and MPC, as well as within WL. Figure- 9 illustrates the distribution of the isocenter difference analysis. MPC vs. PIPSPRO The results indicated that there is a non-significant small difference between PIPSPRO (M = 0.3; SD = 0.06) and MPC (M = 0.3; SD = 0.01), t (29) = 1.5, p = 0.149. The sample difference between the averages of MPC and PIPSPRO is not large enough to be statistically significant. The p-value equals 0.1488, indicating a high chance of a type I error. The test statistic T equals 1.4833, which falls within the 95% region of acceptance. The 95% confidence interval of MPC minus PIPSPRO is [-0.007056, 0.04431]. The observed effect size d is small, 0.27.–Furthermore, based on the Shapiro-Wilk test, MPC minus PIPSPRO follows a normal distribution (p-value = 0.5105).

3.2 MPC vs. MMWL

In contrast, the results showed that there is a significant difference between MMWL (M = 0.2; SD = 0.08) and MPC (M = 0.3; SD = 0.01), t (29) = 5.7, p < 0.001. The sample difference between the averages of MPC and MMWL is large enough to be statistically significant. The p-value equals 0.000004126, indicating a small chance of a type I error. The test statistic T equals 5.6544, which falls outside the 95% region of acceptance. The 95% confidence interval of MPC minus MMWL is [0.04961, 0.1058]. The observed effect size d is large (1.03).-Additionally, based on the Shapiro-Wilk test, MPC minus MMWL follows a normal distribution (p-value is 0.9919).

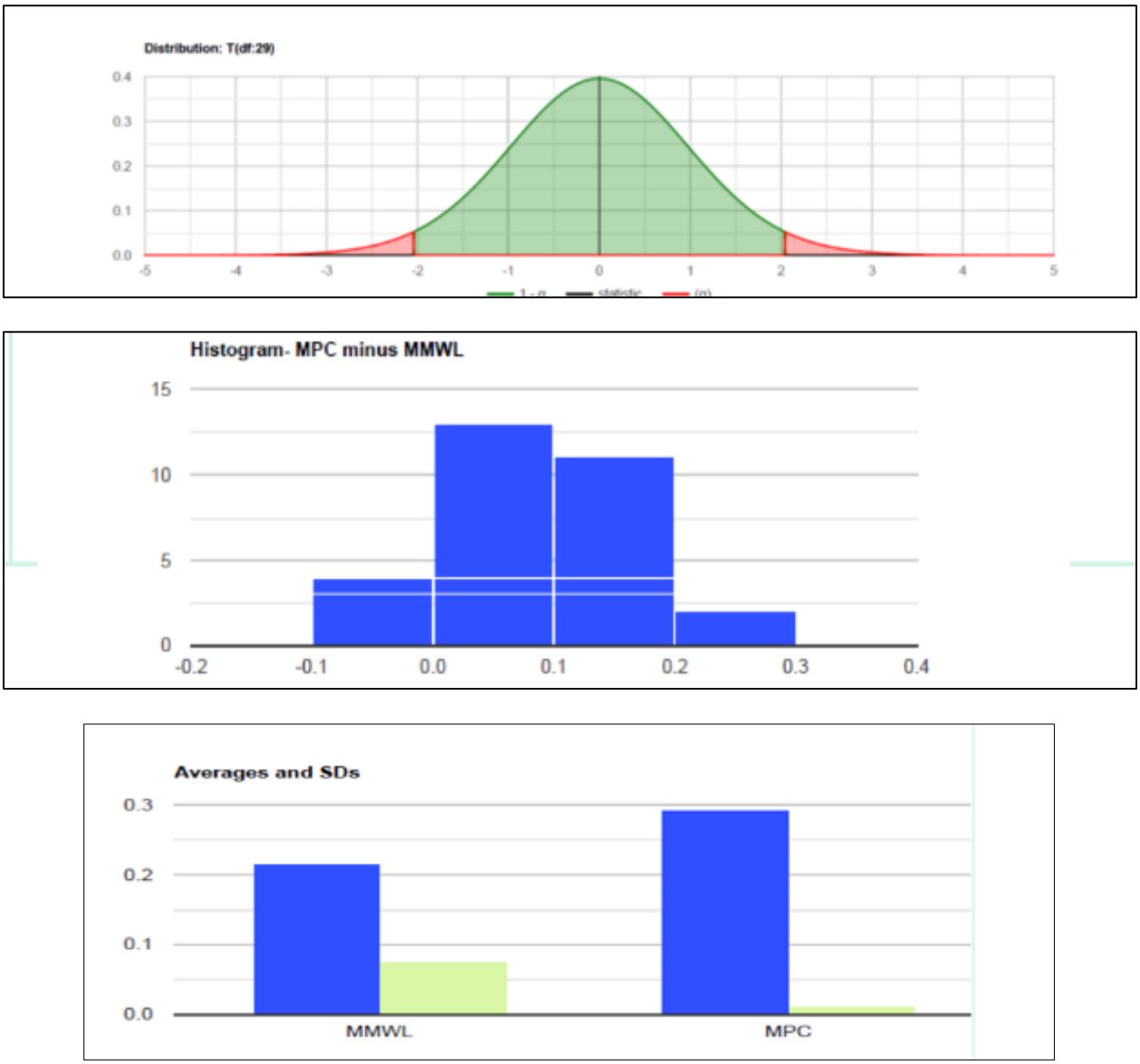

Figure 9b The distribution of the analysis of the isocenter size difference-between MPC and MMWL is shown

3.3 Within WL

The results suggested that there is a significant medium difference between PIPSPRO (M = 0.3; SD = 0.06) and MMWL (M = 0.2; SD = 0.08), t(29) = 3, p =0.005. The sample difference between the averages of MMWL and PIPSPRO is large enough to be statistically significant. The p-value is 0.005386-indicating a small chance of a type I error. The test statistic T equals -3.0083, which falls outside the 95% region of acceptance. The 95% confidence interval of MMWL minus PIPSPRO is [-0.09927, -0.01892]. The observed effect size d is medium (0.55). Moreover, based on the Shapiro-Wilk test, MMWL minus PIPSPRO follows a normal distribution (p-value is 0.7601).

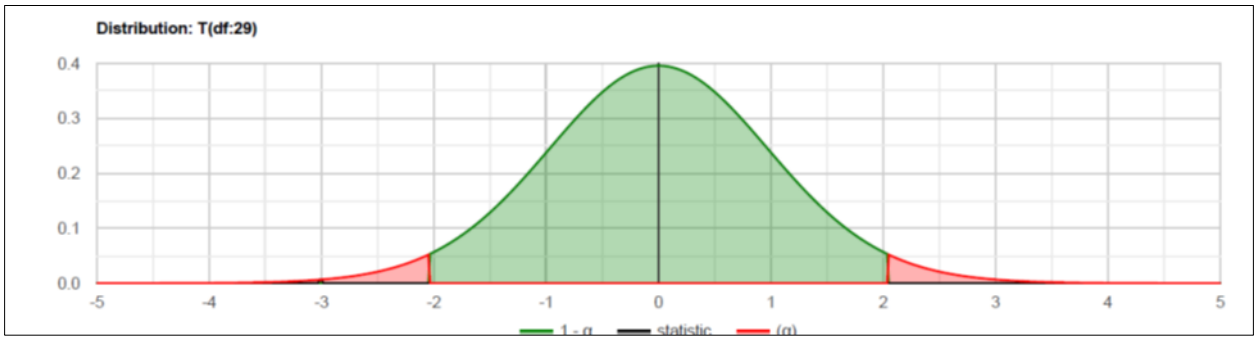

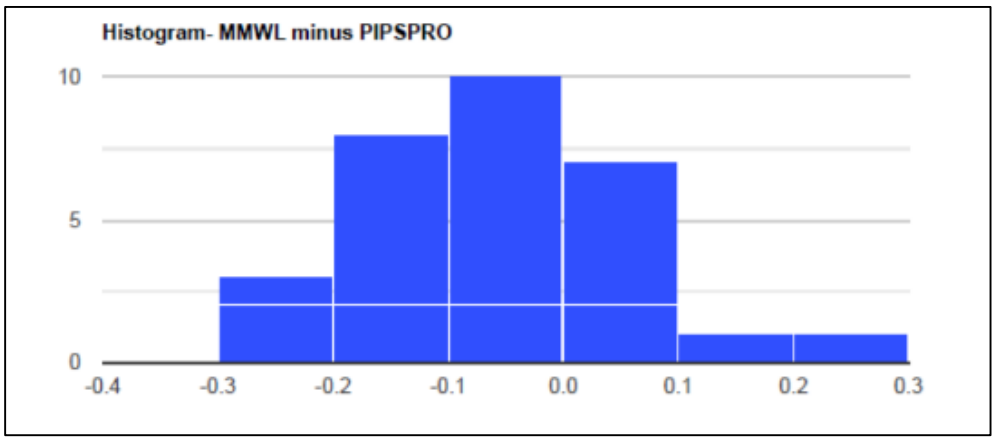

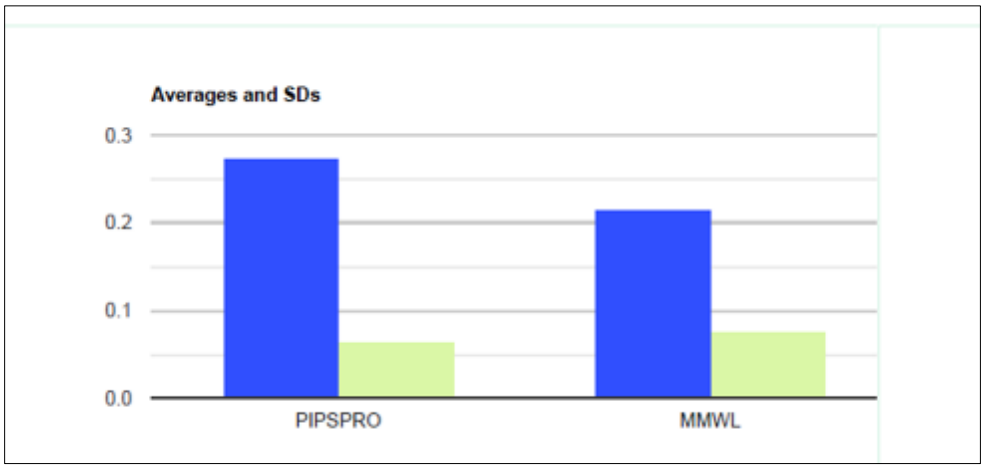

Figure 9c The distribution of the analysis of the isocenter size difference-between MMWL and PIPSPRO is shown

The ROC curve was used to assess the sensitivity and specificity of the isocenter size measurement. The AUC was higher for MPC compared to MMWL (0.8689 ± 0.559; p<0.0001), MMWL vs. PIPSPRO (0.7278 ±0.06572; p<0.0024), and MPC vs. PIPSPRO (0.5622 ±0.08295; p< 0.4077). These results indicate excellent, acceptable, and satisfactory discrimination for MPC vs. MMWL, MMWL vs. PIPSPRO, and MPC vs. PIPSPRO, respectively, when using a 0.5 cut-point for classification.

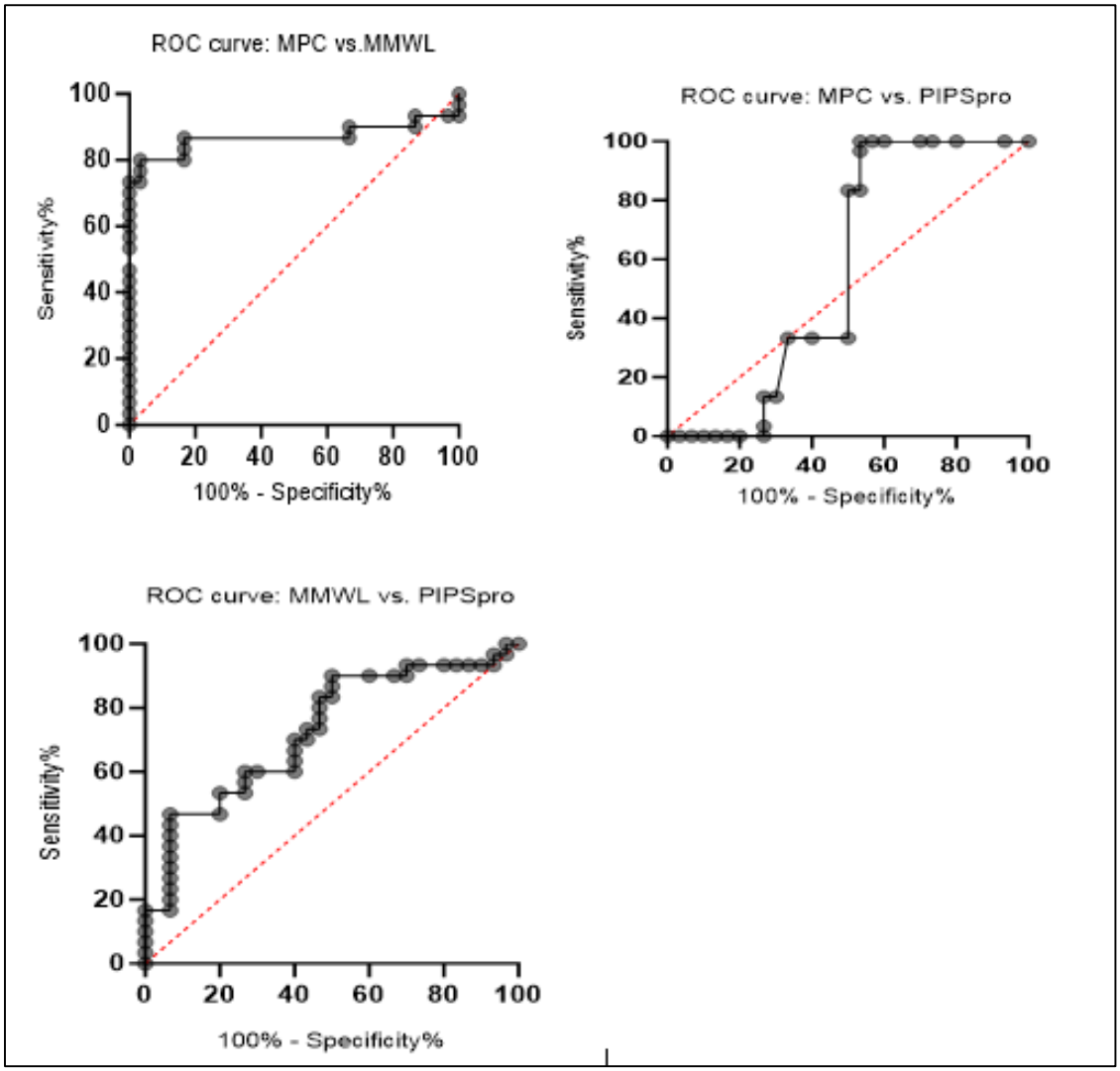

Figure 10 An ROC curve and AUC were generated to assess the mean isocenter size difference using WL and MPC enhanced couch

4 Discussion

In this study, the WL method with cube measurements was compared to the MPC-enhanced couch module. The WL method used two independent pieces of software: one with a defined field size by the MLC and the other with jaw modeling at different gantry, collimator, and couch angles. The study investigated the isocenter size discrepancies between MPC and WL modalities, as well as within WL.

The isocenter size for MPC was found to be 0.293 ± 0.0105 mm, while the WL isocenter discrepancy was very small. The MMWL and PIPISPRO isocenter sizes were 0.2096 ± 0.0703 mm and 0.2736 ± 0.065 mm, respectively. The coefficient of variation (CV%) for MPC, MMWL, and PIPSPRO were 3.58%, 33.5%, and 24%, respectively. Smaller CV% values indicate more precise estimates.

A paired t-test showed that there was a non-significant, small difference between PIPSPRO (M = 0.3; SD = 0.06) and MPC (M = 0.3; SD = 0.01), t (29) = 1.5, p = 0.149. However, there was a significantly large difference between MMWL (M = 0.2; SD = 0.08) and MPC (M = 0.3; SD = 0.01), t (29) = 5.7, p < 0.001, when tested with the same cubic phantom. The results of the WL test showed that there was a significant, medium difference between PIPSPRO (M = 0.3; SD = 0.06) and MMWL (M = 0.2; SD = 0.08), t (29) = 3.0, p = 0.005. The mean difference normality, based on the Shapiro-Wilk test (α = 0.05), followed the normal distribution in this report.

Differences between MPC and WL tests may be due to the phantom mobility during couch displacement compared to the MPC phantom docked in the mount, as well as the WL phantom composed of tungsten carbide BBs, which could result in streaking artifacts. Additionally, Chang et al. [6] suggested that minor distortion or blurring may have occurred due to the embedded radio-opaque marker. In contrast, the Isocal has 16 BBs and a stationary phantom placed near the isocenter, which takes into account collimator uncertainty and gantry sag in its estimate of the treatment isocenter. Hao et al. [7] investigated the monitor unit during cube irradiation and suggested that the ball bearing becomes more detectable as MU increases since most of the statistical noise in pixel values has been washed out to reduce the impact of statistical deviations in phantom measurements due to the cube composition. It is well known that inadequacies in linac gantry rotation are caused by the strong pull of gravity, resulting in slight deviations of the isocenter during treatment. Errors may occur due to gantry sag. The mechanical instabilities of the jaws can cause certain uncertainties, particularly during gantry rotation, when gravity tends to alter jaw positions, consequently modifying the center of radiation fields. It is important to note that mean differences within WL could be the result of different algorithms and resolutions used.

Prospective work could evaluate the use of noise- reduction algorithms and Hough Space transform to achieve sub-pixel resolution. Additionally, one could replicate Rowshanfarzad et al.'s [8] work by conducting a WL test using cine-EPID images during gantry, collimator, and couch angle movements.

In fact, the field size was modeled with MLC for MMWL and jaw size for PIPSPRO, purposely to demonstrate the capture of the entire ball bearing, which is vital in minimizing error in isocenter size measurement. The statistical divergence between methods is clinically insignificant, as indicated by the Bland-Altman limits of agreement. A criterion of ±1.0 mm for geometrical accuracy was recommended by the AAPM for SRS treatment, in accordance with this study, irrespective of the method, software, and phantom.

Our WL results agreed well with those from EPID-based systems using a global thresholding technique, which had an accuracy of 0.3 mm but was prone to noise. Our results are similar to those of Tsai et al. [9], who employed a double convolution method with 0.1 mm accuracy, and Ma et al. [10], who used the Sobel edge detection filter through Hough transform with 0.02 mm accuracy but was subject to a slow process and sensitivity to noise and size. The utilization of different phantoms, such as Quasar, was explored by Schreibmann et al. [11], who found an accuracy of 0.2 mm using the Canny edge detection filter and transformation but was susceptible to noise.

Furthermore, the primary sources of uncertainty are due to the couch treatment. The couch sag is mainly dependent on the couch angle during rotation. An improved quality assurance of the couch could alleviate the effect of rotation and mechanical misalignment, in combination with a meticulous preventive maintenance inspection (PMI) of the couch. The PMI should include, but not be limited to, the inspection and lubrication of the lift drive, LNG/LAT carriage rails, longitudinal encoder and cables, perfect pitch, and turntable.

The off-axis MMWL test reliably assesses the alignment of off-axis positions, the radiation field at those positions, and the cumulative effect of each rotation compared to a traditional QA procedure at fixed points.

There are some drawbacks to this study. Firstly, the data obtained over a month cannot explain long-term stability. Secondly, periodical PMI for couch stability is performed quarterly.

5 Conclusion

In conclusion, this work has thoroughly demonstrated an exhaustive analysis of the WL test with multiple off-axis targets and MPC for SRS/SBRT pretreatment QA. The congruence between the isocenter with MPC and WL using cubes with or without MLC has been thoroughly investigated and corroborated for SRS/SBRT, which requires a stringent tolerance of 1.0 mm. The WL method also provides independent verification of the MPC calibrations.

References

[1] Klein E (2010) Tu-b-203-01: QA of radiation delivery systems: tg-142 quality assurance of medical accelerators. Med Phys 37(6 Part 15):3373–3374. https://doi.org/10.1118/1.3469182

[2] Solberg TD et al (2012) Quality and safety considerations in stereotactic radiosurgery and stereotactic body radiation therapy: executive summary. Pract Radiat Oncol 2(1):2–9. https://doi.org/10.1016/j.prro.2011.06.014

[3] Hubert Szweda Kinga Graczyk, Dawid Radomiak, Krzysztof Matuszewski , Bartosz Pawałowski : Comparison of three different phantoms used for Winston-Lutz test with Artiscan software. Reports of Practical Oncology and Radiotherapy 25 (2020) 351–354)

[4] Anton Eagle, Mike Tallhamer, Justin Keener, Sarah Geneser A simplified and effective off-axis Winston–Lutz for single-isocenter multi-target SRS Volume 24, Issue2 February 2023 e13816 https://doi.org/10.1002/acm2.13816

[5] Gao Junfang, Liu Xiaoqian Winston-Lutz-Gao Test on the True Beam STx Linear Accelerator International Journal of Medical Physics, Clinical Engineering and Radiation Oncology, 2019, 8, 9-20. http://www.scirp.org/journal/ijmpcero

[6] Chang J, Yenice KM, Narayana A, Gutin PH. Accuracy and feasibility of cone-beam computed tomography for stereotactic radiosurgery setup. Med Phys. 2007;34(6):2077–84.

[7] Yao Hao, Matthew C. Schmidt, Yu Wu, Nels C. Knutson Portal dosimetry scripting application programming interface (PDSAPI) for Winston-Lutz test employing ceramic balls. Journal of applied clinical medical physics. DOI: 10.1002/acm2.13043 Volume21, Issue11 November 2020 Pages 295-303.

[8] Rowshanfarzad Pejman, Sabet Mahsheed, O'Connor Daryl J, Greer Peter B. Isocentre verification for linac-based stereotactic radiation therapy: review of principles and techniques. J Appl Clin Med Phys. 2011;(November).

[9] Tsai JS. Analyses of multi-irradiation film for system alignments in stereotactic radiotherapy (SRT) and radio-surgery (SRS). Phys Med Biol. 1996; 41(9):1597–620.

[10] Ma L, Boyer AL, Findley DO, Geis PB, Mok E. Application of a video-optical beam imaging system for quality assurance of medical accelerators. Phys Med Biol. 1998; 43(12):3649–59.

[11] Schreibmann E, Elder E, Fox T. Automated quality assurance for image-guided radiation therapy. J Appl Clin Med Phys. 2009;10(1):71–79.